Supplemental Fig. S1

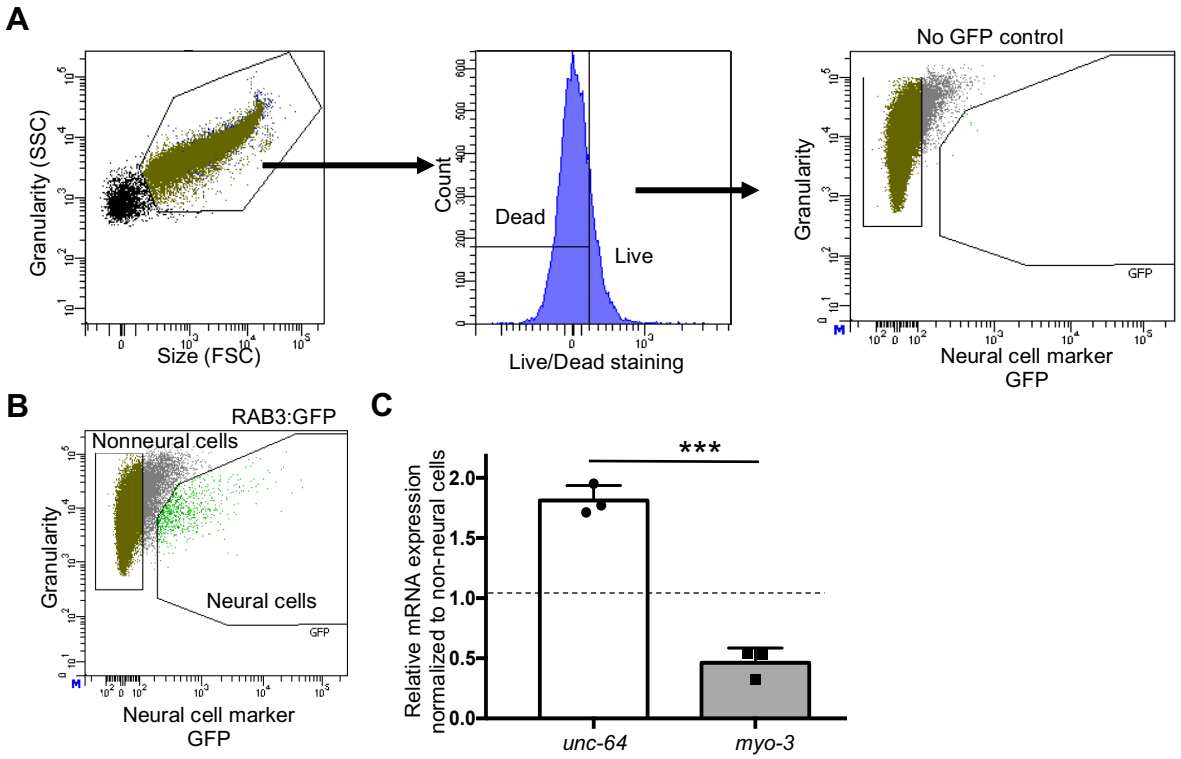

Supplemental Fig. S1: Neural cell isolation from adult worms. (A) GFP expression was driven under the control of the pan-neuronal promoter *rab-3*. Digested adult samples were stained with live/dead strain. Side scatter (SSC) and forward scatter (FSC) were used to select the single cell population, and live/dead strain was used to eliminate dead cells from this population. Non GFP worms were used to define the gating parameters for GFP positive neural isolation. (B) Neural cells from adult animals expressing P*rab-3*::GFP were isolated from non-neural cells. (C) qPCR was used to quantify the expression of neural specific gene *syntaxin* (*unc-64*) and a non-neural gene *myo-3* in isolated neural cells and non-neural cells in three biological replicates. Level of mRNA expression in the non-neural cells was set to 1 (dotted lines) and the significance for enrichment of each gene was calculated using a Student's *t*-test. Three asterisks represent *p*-value < 0.001.

Supplemental Fig. S2

A

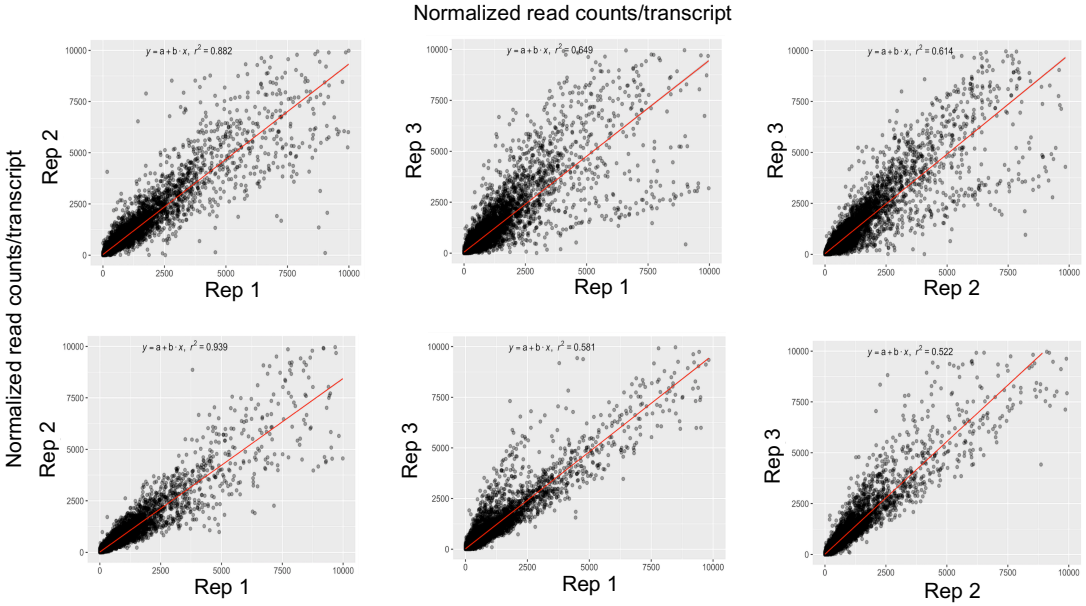

B

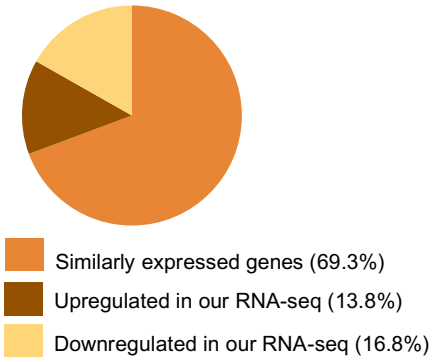

Supplemental Fig. S2: Assessing the reproducibility of the RNA-seq data sets. (A) Pairwise comparisons of biological replicates of RNA-seq from wild-type (top) and *adr-2(-)* adult neurons (bottom). (B) Differential gene expression analysis of adult neural RNA-seq from our lab and (Kaletsky et al. 2018). Expression of 18,630 genes were not significantly different (*P*-adj > 0.05) between three biological replicates of adult RNA seq from both labs. Nearly 17% of the genes (4450) were downregulated (*P*-adj < 0.05, $\log_2$ fold < -0.5), while 13.8% of the genes (3697) were upregulated (*P*-adj < 0.05, $\log_2$ fold > 0.5) in our adult neural RNA-seq compared to adult neural RNA-seq published in (Kaletsky et al. 2018).

Supplemental Fig. S3

A

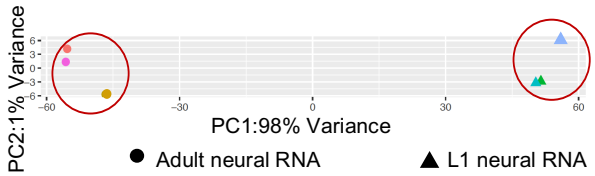

B

Biological process	FDR
Cellular metabolic process (GO:0044237)	4.28E-52
Response to stress (GO:0006950)	7.87E-07
Cell cycle (GO:0007049)	1.09E-06
Reproduction (GO:0000003)	7.31E-05
Developmental process (GO:0032502)	7.94E-05
Response to endoplasmic reticulum stress (GO:0034976)	1.18E-04
Response to unfolded protein (GO:0006986)	1.53E-04
Embryo development (GO:0009790)	1.52E-02
Oogenesis (GO:0048477)	1.59E-02
DNA repair (GO:0006281)	2.78E-02
Cuticle development involved in collagen and cuticulin-based cuticle molting cycle (GO:0042338)	3.44E-02
Response to organic substance (GO:0010033)	4.54E-02

Biological process	FDR
Response to stimulus (GO:0050896)	1.18E-53
Signaling (GO:0023052)	7.10E-53
Developmental process (GO:0032502)	1.86E-31
Locomotion (GO:0040011)	4.14E-23
Nervous system development (GO:0007399)	1.09E-22
Taxis (GO:0042330)	3.07E-18
Cell differentiation (GO:0030154)	3.11E-18
Regulation of signaling (GO:0023051)	3.22E-18
Chemotaxis (GO:0006935)	5.42E-16
Neuron differentiation (GO:0030182)	4.55E-13
Response to abiotic stimulus (GO:0009628)	4.92E-12
Aging (GO:0007568)	1.58E-08
Programmed cell death (GO:0012501)	1.33E-02

C

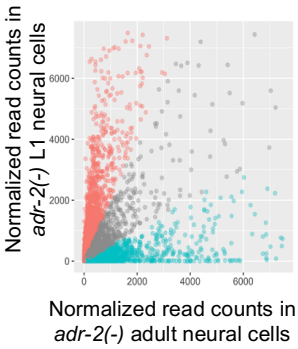

D

Biological process	FDR	Number of genes	Edited in neurons
Cellular metabolic process (GO:0044237)	9.76E-38	237	15
Regulation of developmental process (GO:0050793)	5.34E-09	62	3
Determination of adult lifespan (GO:0008340)	4.53E-07	32	1
Negative regulation of gene expression (GO:0010629)	3.71E-06	41	1
Protein ubiquitination (GO:0016567)	1.10E-05	29	2
Response to stress (GO:0006950)	1.18E-05	72	5
Regulation of signaling (GO:0023051)	1.20E-05	43	4
RNA splicing (GO:0008380)	1.47E-04	10	0
Neuropeptide signaling pathway (GO:0007218)	1.26E-03	38	1
Regulation of response to stimulus (GO:0048583)	2.07E-03	51	4

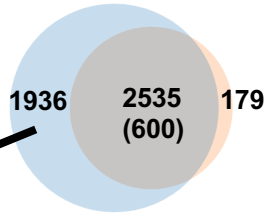

E

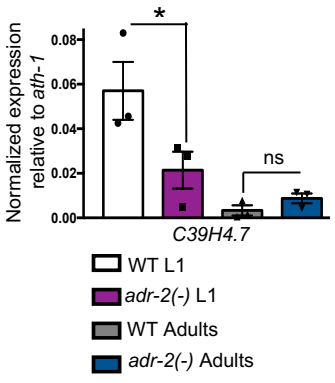

F

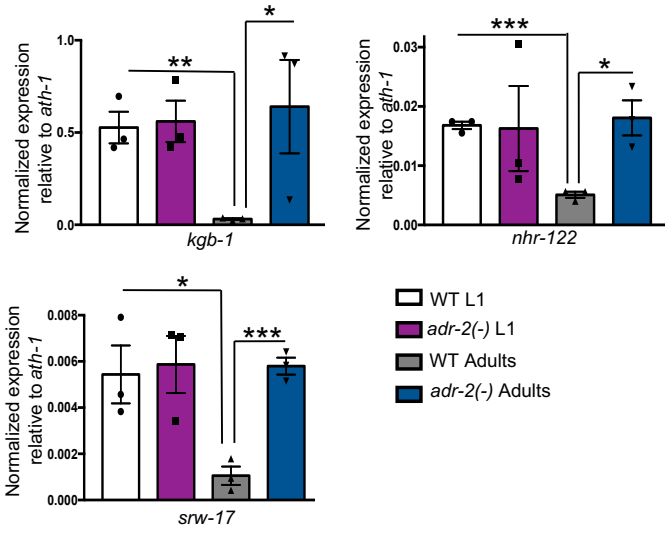

Supplemental Fig. S3: The role of *adr-2* in differential gene expression in neural cells during development. (A) Principle Component analysis of the samples used in differential gene expression in wild-type neural cells during development. Circle represents RNA-seq from wild-type adult neurons, Triangle represents RNA-seq from wild-type L1 neurons, different colors represent biological replicates. (B) Gene ontology analysis of the upregulated (left) and downregulated (right) genes in wild-type adult neurons compared to wild-type L1 neurons using http://geneontology.org/. Enriched categories and respective False discovery rate (FDR) are listed. (C) Differential gene expression analysis of L1 and adult neurons from *adr-2(-)* worms. Red (2714) and blue (4374) dots represent down- (*P*-adj < 0.05, $\log_2$ fold < -0.5) and upregulated (*P*-adj < 0.05, $\log_2$ fold > 0.5) genes in adult neurons compared to L1 neurons. Grey dots represent genes (9362) that are not significant (*P*-adj > 0.05) between three biological replicates of L1 RNA-seq and adult RNA seq. (D) Downregulated genes in adult neural cells compared to L1 neural cells from wild-type (blue circle) and *adr-2(-)* (orange circle) animals were overlapped. Gene ontology analysis of the ADR-2 dependent downregulated genes with the enriched categories and False discovery rate (FDR) listed. (E and F) qPCR validation of downregulated genes. The average of three independent replicates is plotted with error bars representing SEM. Statistical significance was calculated using a Student's *t*-test. One asterisk represents $p < 0.05$, two asterisks represent $p < 0.01$ and three asterisks represent $p < 0.001$ and ns represents $p > 0.05$.

Supplemental Fig. S4

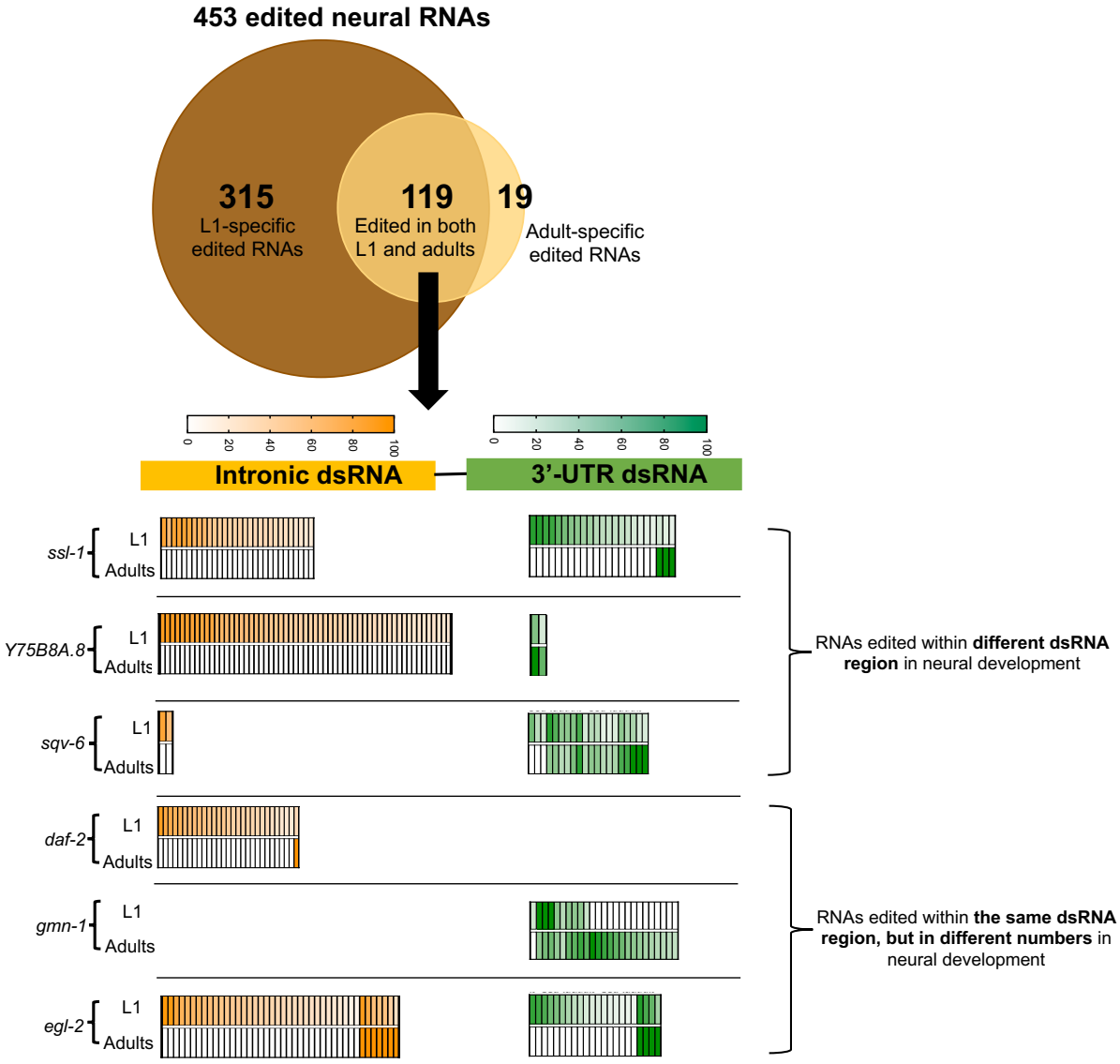

Supplemental Fig. S4: Neural transcripts that are edited throughout development (A) L1 (434) and adult (138) edited transcripts were overlapped to identify transcripts that are edited throughout neural development (119). (B) The top three are representative edited transcripts from the RNAs that are edited within a specific dsRNA region in a stage-specific manner (12 total). Similarly, the bottom three are representative edited transcripts from the mRNAs that are edited within the same dsRNA region throughout development are shown (107 total). Each box within the heatmap represents an individual edited site and the percent editing is represented by color shading.

Supplemental Fig. S5

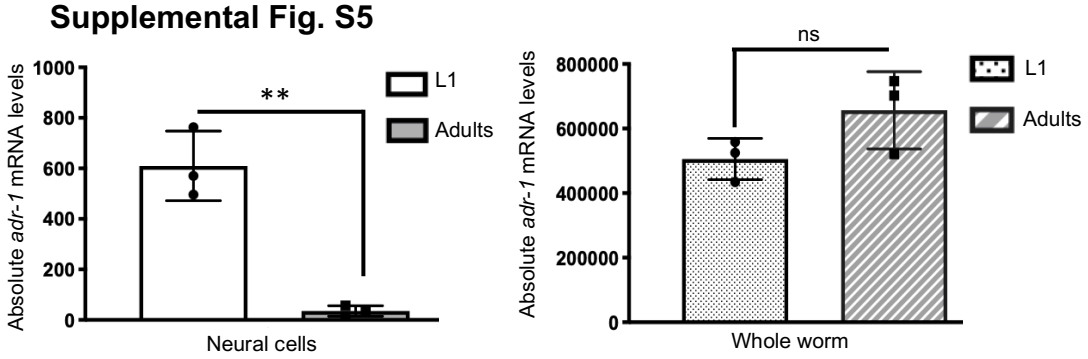

Supplemental Fig 5: *adr-1* mRNA expression during neural development. qPCR was used to quantify *adr-1* expression in neural cells (left) and in whole worm lysate (right) for both L1 and adults. The average of three independent replicates is plotted with error bars representing SEM. Statistical significance was calculated using a Student's *t*-test. Two asterisks represent $p < 0.01$ and ns represents $p > 0.05$.

Supplemental Fig. S6

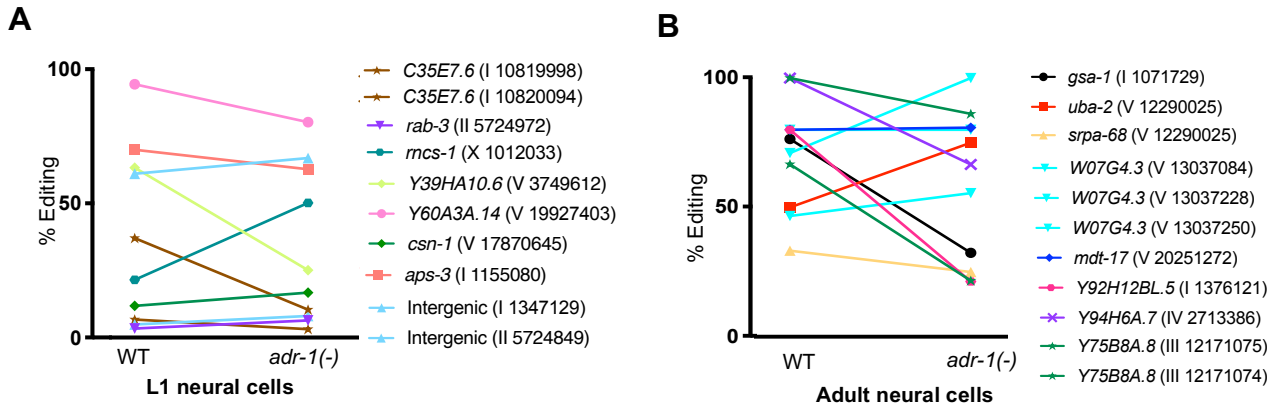

Supplemental Fig. S6: Editing at a majority of the sites in constitutively expressed neural transcripts did not increase in the absence of *adr-1* in the adult stage. (A) Neural RNA-seq data was used to plot the editing levels of randomly selected sites from L1 neural cells in the presence and absence of *adr-1* ($p > 0.05$, pairwise comparison using Two-way ANOVA). (B) Neural RNA-seq data was used to plot the editing levels of representative sites (shown in Fig. 5E) in adult neural cells in the presence and absence of *adr-1* ($p > 0.05$, pairwise comparison using Two-way ANOVA).

Supplemental Fig. S7

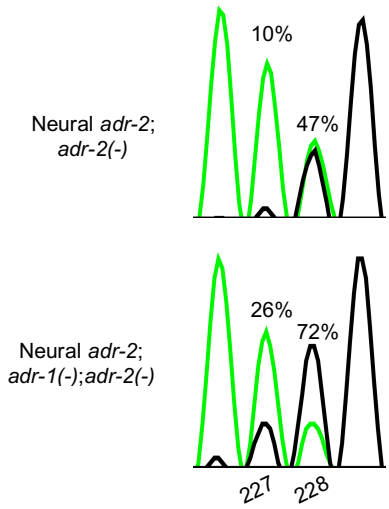

Supplemental Fig. S7: Expression of functional ADR-2 within the neural cells. Sanger sequencing chromatograms of cDNA amplified from *Y75B8A.8* reporter RNA in L1 stage transgenic worms expressing neural ADR-2 in the presence and absence of *adr-1*. Editing sites are listed below the chromatogram. The nucleotides at each position are represented with a different color (Green = Adenosine, Black = Guanosine). The percentage of editing at sites 227 and 228 are given above the chromatogram.

Supplemental Fig. S8

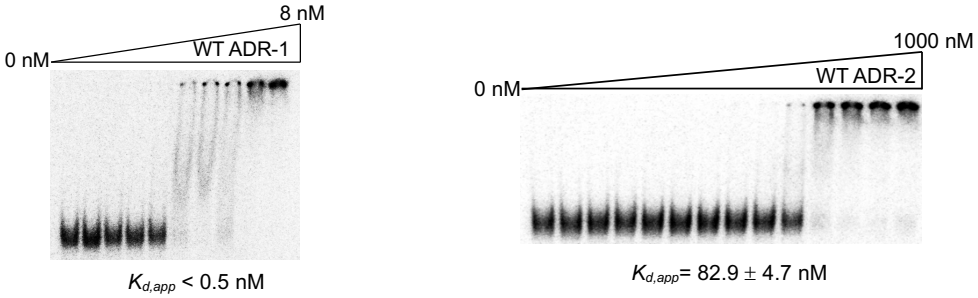

Supplemental Fig. S8: Compared to ADR-2, ADR-1 has stronger affinity to *Y75B8A.8* dsRNA. Increasing amounts of WT ADR-1 (left) and ADR-2 (right) were mixed with ^{32}P-labeled 78 bp dsRNA from the *Y75B8A.8* 3′ UTR (20 pM) and incubated on ice for 30 min. Complex formation was analyzed by native gel electrophoresis. Initial and final protein concentrations are marked above gel with adjacent lanes representing a 2-fold difference in protein concentration. The dissociation constant ($K_{d,\ app}$) was calculated from the binding curve generated for specific binding using a Hill slope. These values are similar to those reported for ADR-1 and ADR-2 binding to dsRNA from the *lam-2* 3′ UTR (Rajendren et al. 2018)

References

Kaletsky R, Yao V, Williams A, Runnels AM, Tadych A, Zhou S, Troyanskaya OG, Murphy CT. 2018. Transcriptome analysis of adult Caenorhabditis elegans cells reveals tissue-specific gene and isoform expression. *PLoS Genet* **14**: e1007559.

Rajendren S, Manning AC, Al-Awadi H, Yamada K, Takagi Y, Hundley HA. 2018. A protein-protein interaction underlies the molecular basis for substrate recognition by an adenosine-to-inosine RNA-editing enzyme. *Nucleic Acids Res* **46**: 9647-9659.